Impact of cavitation on lesion formation induced by high intensity focused ultrasound*

Pengfei Fan(范鹏飞)[1], Jie Yu(于洁)[1], Xin Yang(杨鑫)[1], Juan Tu(屠娟)[1,†], Xiasheng Guo(郭霞生)[1], Pintong Huang(黄品同)[2], and Dong Zhang(章东)[1,3,‡]

[1] *Key Laboratory of Modern Acoustics (Nanjing University), Ministry of Education, Nanjing University, Nanjing* 210093, *China*
[2] *Department of Ultrasound, The Second Affiliated Hospital of Zhejiang University School of Medicine, Hangzhou* 310009, *China*
[3] *The State Key Laboratory of Acoustics, Chinese Academy of Science, Beijing* 100080, *China*

(Received 26 December 2016; revised manuscript received 18 February 2017; published online 6 April 2017)

High intensity focused ultrasound (HIFU) has shown a great promise in noninvasive cancer therapy. The impact of acoustic cavitation on the lesion formation induced by HIFU is investigated both experimentally and theoretically in transparent protein-containing gel and *ex vivo* liver tissue samples. A numerical model that accounts for nonlinear acoustic propagation and heat transfer is used to simulate the lesion formation induced by the thermal effect. The results showed that lesions could be induced in the samples exposed to HIFU with various acoustic pressures and pulse lengths. The measured areas of lesions formed in the lateral direction were comparable to the simulated results, while much larger discrepancy was observed between the experimental and simulated data for the areas of longitudinal lesion cross-section. Meanwhile, a series of stripe-wiped-off B-mode pictures were obtained by using a special imaging processing method so that HIFU-induced cavitation bubble activities could be monitored in real-time and quantitatively analyzed as the functions of acoustic pressure and pulse length. The results indicated that, unlike the lateral area of HIFU-induced lesion that was less affected by the cavitation activity, the longitudinal cross-section of HIFU-induced lesion was significantly influenced by the generation of cavitation bubbles through the temperature elevation resulting from HIFU exposures. Therefore, considering the clinical safety in HIFU treatments, more attention should be paid on the lesion formation in the longitudinal direction to avoid uncontrollable variation resulting from HIFU-induced cavitation activity.

Keywords: high intensity focused ultrasound, tissue lesion, acoustic cavitation

PACS: 43.25.Yw, 43.35.Wa, 43.80.+p **DOI:** 10.1088/1674-1056/26/5/054301

1. Introduction

High intensity focused ultrasound (HIFU) is an emerging noninvasive therapeutic modality to treat tumors, in which ultrasound energy is locally absorbed in a millimeter-size focal region to induce tissue necrosis without damaging intervening tissues.[1] During HIFU treatment, large rarefaction pressure amplitudes may place the surrounding tissue under sufficient tension to form cavities filling with gas and vapor, and subsequent ultrasonic excitation will cause these bubbles to generate acoustic cavitation.[2–4] It has been demonstrated that the presence of acoustic cavitation at the ultrasound focal region can lead to substantially higher rates of tissue heating.[5–9] As a result, this enhanced heating rate can promote the growth of lesions whose features depend on the exciting ultrasonic parameters.[10,11] On the other hand, scattering from cavitation bubbles also produces a region with increased echogenicity on the B-mode image which may contribute to real-time monitoring of HIFU treatment.[10,12]

Considering that most of HIFU treatments operate at very high acoustic intensities that lead to a large temperature rise,[10,13] the safety of HIFU treatment needs to be ensured. One solution to improve the safety of HIFU is introducing some effective and accurate monitoring method, such as ultrasound image-guidance[12–18] and MRI-guidance.[19–23] However, there still exist some problems, like time delay for the MRI image system and low image resolution of the ultrasound system. The alternative method is to investigate the principle of the interaction between high intensity ultrasound and tissue. Generally speaking, HIFU is a multi-parameter physical system where there are several parameters that can influence the formation of a lesion, such as acoustic pressure, pulse length, period repetitive frequency (PRF), and so on. Khokhlova *et al*. indicated that the nonlinear acoustic enhancement of lesion production could become pronounced in a narrow zone around the focal axis where shock waves formed.[22] Furthermore, the heating duration and absorbed power density were also important factors in lesion forming.[24]

This work aimed to systematically investigate how acoustic cavitation influences the temperature rise and lesion formation in both in vitro and ex vivo studies. Firstly, the temperature elevation and lesion formation were simulated by utilizing Khokhlov–Zabolotskaya–Kuznetsov (KZK) and the

*Project supported by the National Natural Science Foundation of China (Grant Nos. 11374155, 11674173, 11474001, 11474161, 81627802, and 81527803), and Qing Lan Project, China.

†Corresponding author. E-mail: juantu@nju.edu.cn
‡Corresponding author. E-mail: dzhang@nju.edu.cn

© 2017 Chinese Physical Society and IOP Publishing Ltd

Pennes bioheat transfer model with varied ultrasonic exciting parameters. Then, the experiments in gel phantom and *ex vivo* liver samples were conducted to compare with the simulated results. Meanwhile, a B-mode scanner was used to quantitatively monitor the generation of acoustic cavitation for the following analysis. The results of the present work would be beneficial for better understanding the role of cavitation on lesion formation and providing a better guidance for the design of HIFU treatment strategy.

2. Methods

2.1. Acoustical and thermal models

The widely used nonlinear KZK equation was used to describe the nonlinear ultrasound propagation in tissue, which was written as[25,26]

$$\frac{\partial^2 p}{\partial z \partial \tau} = \frac{c_0}{2}\Delta_\perp p + \frac{b}{2\rho_0 c_0^3}\frac{\partial^3 p}{\partial \tau^3} + \frac{\beta}{2\rho_0 c_0^3}\frac{\partial^2 p^2}{\partial \tau^2}, \tag{1}$$

where the three terms on the right side represent diffraction, attenuation, and nonlinear effects; p, ρ_0, c_0, b, and β are respectively the acoustic pressure , the ambient density, the speed of sound, the dissipation parameter, and the coefficient of nonlinearity; the Laplacian operator is $\Delta_\perp = \partial^2/\partial x^2 + \partial^2/\partial y^2$ in rectangular coordinates; $\tau = t - z/c_0$ is the retarded time and z stands for the coordinate along the beam axis. Using a combined modeling and measurement calibration technique[27] as the boundary conditions, the equation can be solved in the frequency domain using a finite difference algorithm.[25] In the frequency domain, the sound pressure is represented in the form of a Fourier series expansion

$$p(z,r,t) = \sum_{n=-\infty}^{+\infty} C_n(z,r)\exp(\mathrm{j}n\omega\tau), \tag{2}$$

where $C_n(z,r)$ is the complex amplitude of the n-th harmonic component at point (z,r) and ω is the fundamental frequency of the HIFU pulses.

According to the heating effect of HIFU, there will be a temperature rise in target region. In soft tissues, the temperature rise is well modeled by the Pennes bioheat transfer equation,[28,29] which is described as

$$\frac{\partial T}{\partial t} = \frac{k}{\rho_0 C}\nabla^2 T + \frac{Q}{\rho_0 C}, \tag{3}$$

where T and ρ_0 are the temperature and density of gel; C and k represent heat capacities and thermal conductivity of tissue; the heat deposition source related to the acoustic field is

$$Q = \frac{1}{\rho_0 c_0}\sum_{n=1}^{N} 4\alpha_0 n^\mu |C_n|^2,$$

where $\alpha_0 = \omega^\mu b/2\rho_0 c_0^3$ is the attenuation coefficient of the fundamental harmonic and N stands for the highest order harmonic number in the calculation. Equation (3) can be separated into three one-dimensional partial difference equations in rectangular coordinates to simulate the temperature variations along individual directions:[13]

$$\left.\frac{\partial T}{\partial t}\right|_z = \frac{k}{\rho_0 C}\frac{\partial T}{\partial z^2} + \frac{Q}{\rho_0 C},$$
$$\left.\frac{\partial T}{\partial t}\right|_y = \frac{k}{\rho_0 C}\frac{\partial T}{\partial y^2}, \quad \left.\frac{\partial T}{\partial t}\right|_x = \frac{k}{\rho_0 C}\frac{\partial T}{\partial x^2}. \tag{4}$$

With the boundary condition

$$\frac{\partial^2 T}{\partial x^2}|_{x=0,x=X_{\max}} = \frac{\partial^2 T}{\partial y^2}|_{y=Y\max} = \frac{\partial^2 T}{\partial z^2}|_{z=0,z=Z_{\max}} = 0$$

and $\frac{\partial T}{\partial y}|_{y=0} = 0$, the equation (3) can be calculated.

According to the distribution of the temperature, the thermal dose is calculated by[30]

$$t_{43} = \int_{t=0}^{t=t_{\mathrm{f}}} R^{43-T(t)}\,\mathrm{d}t, \tag{5}$$

where t_{43} is the thermal dose equivalent time at 43 °C and t_{f} is the time of the end of heating. It is noticed that 240 min at 43 °C is commonly considered as the threshold for lesion formation in soft tissue.[13]

In this simulation, it is assumed that gel is homogeneous in terms of both acoustic and thermal properties. Up to the first 40 harmonics were used with a grid spacing of $\mathrm{d}r = 0.1$ mm, $\mathrm{d}z = 0.04$ mm and a time step of $\mathrm{d}t = 0.01$ s as a compromise between numerical accuracy and computational cost. The values of the physical constants used for acoustic and thermal modeling are $\rho_0 = 1040\ \mathrm{kg\cdot m^{-3}}$, $c_0 = 1542\ \mathrm{m\cdot s^{-1}}$, $C = 4500\ \mathrm{W\cdot s\cdot m^{-3}\cdot {}^\circ C^{-1}}$, $k = 0.6\ \mathrm{W\cdot m^{-1}\cdot {}^\circ C^{-1}}$, $\alpha = 2.3\ \mathrm{Np\cdot m^{-1}}$, $\beta = 4.2$, $\mu = 1.1$ for gel phantom and $\rho_{\mathrm{b}} = 1050\ \mathrm{kg\cdot m^{-3}}$, $c_{\mathrm{b}} = 1596\ \mathrm{m\cdot s^{-1}}$, $C_{\mathrm{b}} = 3800\ \mathrm{W\cdot s\cdot m^{-3}\cdot {}^\circ C^{-1}}$, $k_{\mathrm{b}} = 0.6\ \mathrm{W\cdot m^{-1}\cdot C^{-1}}$, $\alpha_{\mathrm{b}} = 4.5\ \mathrm{Np\cdot m^{-1}}$, $\beta_{\mathrm{b}} = 6$, $\mu_{\mathrm{b}} = 1.266$ for liver samples, which are similar to the reported data.[31,32]

2.2. Experimental methods

2.2.1. Sample preparation

An optically transparent polyacrylamide gel containing egg white was used here as a tissue-mimicking phantom. Every 100 ml mixed solution consists of 42 ml degassed water, 30 ml egg white, 26.2 ml aqueous solution of 40% (w/v) acrylamide, 0.5 ml 10% ammonium peroxodisulfate, and 0.3 ml TEMED. The recipe was similar to that proposed by Takegami *et al.*[33] The egg white was filtrated 3 times by a stainless steel screen cloth with 0.045-mm-diameter holes and centrifuged for 10 min at 3000 rpm. The liquid was placed in a refrigerator until cooled down to 43 °C to avoid the degeneration induced by heat released during polyreaction. The gel was finally confined via polymerization reaction in a $10\times10\times5\ \mathrm{cm^3}$ sample holder.

The *ex vivo* tissue samples used in this work were freshly excised bovine liver from a local slaughterhouse on the day of

the experiments. The samples were cut into a uniform size of $10 \times 10 \times 5$ cm^3, placed into the sample holder, and then immersed in degassed water, with the HIFU focus 1.5-cm away from the front surface of the samples.

2.2.2. Experimental setup

Figure 1 illustrates the diagram of the experimental setup. A 1.12-MHz single-element focused piezoelectric transducer (10.0 cm focal length, 10.0 cm aperture diameter) was used as the HIFU transmitter for all the measurements. An arbitrary waveform generator (33250A, Agilent, Santa Clara, CA, USA) was used to produce tone-burst signals with 1.12-MHz driving frequency, 100-Hz PRF, and 20-cycle pulse length for ultrasound field measurements or various pulse lengths for temperature rise and lesion measurements. Then the signals were used to drive the ultrasound transmitter via an impedance matching network, after being amplified by an RF-amplifier (A150, ENI, Rochester, NY, USA). The transmitted signals were measured using a calibrated broadband needle hydrophone (TNU0001A, NTR, Seattle, WA, USA) with an active diameter of 0.6 mm and an upper frequency limit of 20 MHz.

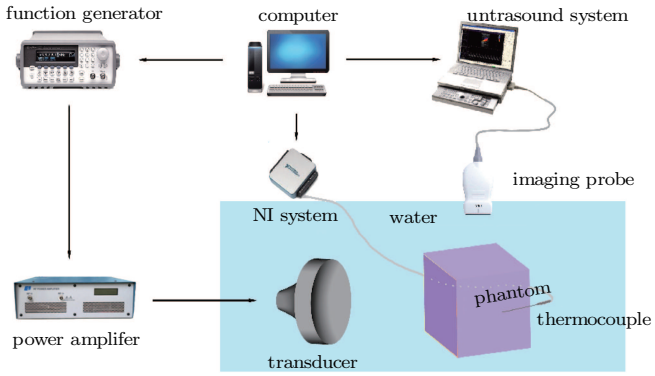


Fig. 1. (color online) Schematic diagram of experimental apparatus which includes the HIFU exposure system, B-mode imaging system, and temperature measuring system.

During the experiment, a 5C2-A scan head of the B-mode ultrasound scanner (Terasont3000, Dvision of Teratech Co., Burlinton, MA, USA) was utilized to monitor HIFU-induced cavitation. In addition, the scan head was placed in a thin plastic sleeve (ATL/Philips, Bothell, WA, USA) which was filled with ultrasound coupling gel to stop cavitation bubbles generating on the surface of the scan head. Then the scan head was moved to the focal plane by a linear 3-axial mechanic scanning system (Newport ESP7000, USA) controlled by a PC via a Labview software (NI Corp., TX, USA). HIFU-induced cavitation area could be observed using the B-mode scanner, and the B-mode images were recorded in the computer for the following imaging processing analysis. To detect the temperature in the focal region, a T-type embedded fine-needle thermocouple (diameter 0.25 mm, TJ72-CASS-010G-4, Omega, Engineering Inc., Stamford, CT) was used. A data collector (NI 9214, National Instruments, Austin, TX, USA) was connected to the thermocouple, recording the data at a sample frequency of 10 Hz under the control of the Labview program. The data files were then downloaded to the computer for further processing.

2.2.3. Experimental protocols

To create lesions, the gel/tissue samples were exposed to HIFU pluses with two sets of ultrasonic exciting parameters: (i) varied acoustic pressure amplitude ranging from 6.25 MPa to 9.92 MPa with a fixed pulse length of 2000 cycles and (ii) varied pulse lengths ranging from 2000 to 6000 cycles with a fixed acoustic pressure of 7.5 MPa. It should be pointed out that, due to the limited resource of fresh liver samples, the acoustic pressure of 6.25 MPa was not included in the *ex vivo* experimental protocol. After HIFU exposure, the cross-section images in the lateral and longitudinal planes were captured by a digital camera (NEX-6, SONY, Japan). Then, the contour outlines of cross-sectional lesions were obtained by using the software of Image J (NH, USA). Referring to the ratio between the pixel and actual length, the cross-sectional lesion areas were finally quantified according to the number of pixels within the contours. Three replicated experiments were performed for each parameter set.

2.2.4. B-mode image analysis

There are always bright mask strips in the B scan image of cavitation, because of the interference between B-mode interrogation signals and HIFU pulses. Therefore, a special imaging progressing algorithm was needed to eliminate the interference mask strips from the images. This progressing algorithm included the following steps: (i) wiping off background noise signals through histogram equalization and contrast enhancement processes; (ii) applying a modified image correlation process to these images based on grayscale matching criteria; and (iii) smoothing the image with a 5×5 Gaussian filtering process. Finally, a series of stripe-wiped-off pictures were obtained so that the area of cavitation region with a distinct edge could be quantified in terms of pixels.

Following the above procedure, the images will be eventually converted to binary images by applying an appropriate intensity threshold (e.g., the threshold was chosen as 12.5% higher than the background gray-scale value in the first B-mode image). [12] The edge of the cavitation region can be detected so that the area of the region of interest can be quantified in terms of pixels. Figure 2 illustrate a typical sample of B-scan images before and after imaging processing.

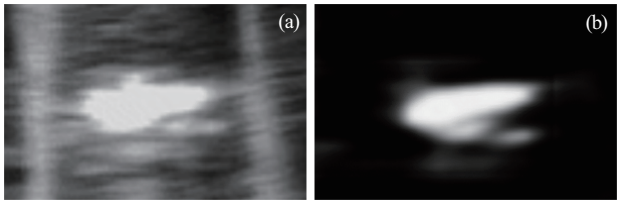


Fig. 2. Comparison between B scan image before (a) and after (b) imaging processing.

3. Results and discussion

3.1. HIFU-induced lesion in gel

With the gel being exposed to HIFU pulses, an asymmetric tadpole-like lesion was generated, which agreed with previous reports.[10] Figures 3 and 4 show the cross-section images of lesions generated by the HIFU with varied acoustic pressures at fixed pulse length of 2000 cycles and with varied pulse lengths at constant acoustic pressure of 7.5 MPa, respectively. It is obvious that lesions with a larger area are induced at larger acoustic pressure or pulse length. However, the acceleration rate of the lesion area exhibits different behaviors as the pulse length or acoustic pressure amplitude increases. In Fig. 3, both the areas of lateral and longitudinal cross-section of the lesion have significant enhancement as the acoustic pressure amplitude increases from 6.25 to 9.92 MPa, while in Fig. 4 only the area of the longitudinal section of lesion increases significantly with the increasing pulse length from 2000 to 6000 cycles.



Fig. 3. (color online) Lateral and longitudinal cross-section images of the lesions in the gel phantoms exposed to HIFU with the fixed pulse length 2000 cycles and varied acoustic pressures: (a) 6.25 MPa, (b) 7.5 MPa, (c) 8.75 MPa, and (d) 9.92 MPa.

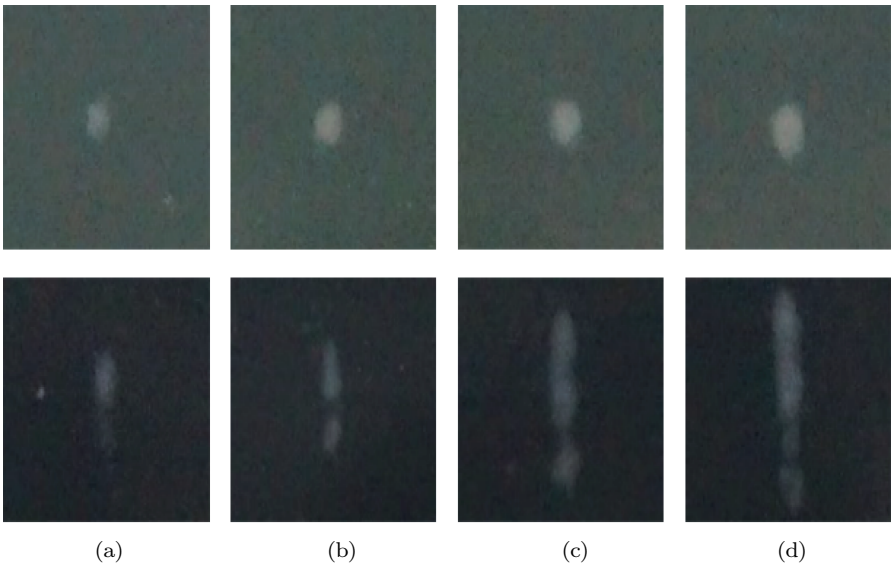


Fig. 4. (color online) Lateral and longitudinal cross-section images of the lesions in the gel phantoms exposed to HIFU with the fixed acoustic pressure of 7.5 MPa and varied pulse lengths: (a) 2000 cycles, (b) 3000 cycles, (c) 4000 cycles, and (d) 6000 cycles.

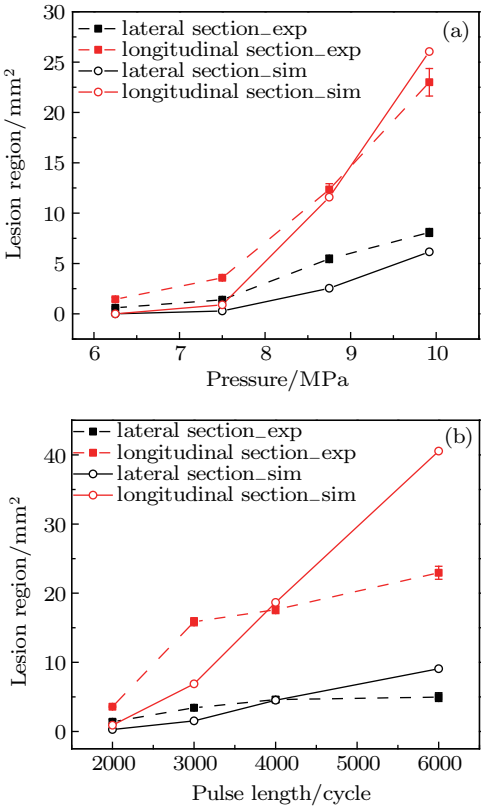


Fig. 5. (color online) Calculated and measured lesion area in the gel phantoms. Lateral and longitudinal lesion area generated by HIFU (a) with varied acoustic pressure and the fixed pulse length of 2000 cycles, and (b) with varied pulse length and fixed acoustic pressure of 7.5 MPa.

To quantitatively investigate the change of lesion area with the ultrasonic exciting parameters, the areas of the longitudinal and the lateral section were quantified after image processing. Figure 5 shows lesion areas of the longitudinal and lateral section generated at a fixed pulse length of 2000 cycles and at a fixed acoustic pressure amplitude of 7.5 MPa, where the solid lines indicate the simulation results and the dotted lines represent the measured data. As shown in Fig. 5, both the calculated and measured lateral cross-section areas of the lesion grows gradually as the acoustic pressure amplitude increases from 6.25 to 9.92 MPa or as the pulse length increases from 2000 to 6000 cycles. However, unlike the lateral cross-section area, a rapid accelerating rate can be observed for the longitudinal cross-section area in both the experimental and simulated results. More importantly, more obvious discrepancies are observed for the longitudinal cross-section area between calculated and measured ones, especially when the acoustic driving pressure and pulse length reach relatively high values. The reason for this phenomenon will be discussed later.

3.2. HIFU-induced lesion in liver tissue samples

As the liver is not transparent, the pictures of longitudinal and lateral cross-section lesions in the liver samples cannot be acquired at the same time. Therefore, only longitudinal cross-section images of the lesions were obtained. Based on the assumption that the lateral cross-section of the lesion should have an approximately circular contour, its diameter could be estimated according to the largest lateral dimension measured in the longitudinal cross-section image (e.g., the segment d marked in Figs. 6 and 7). Figures 6 and 7 illustrate the cross-section images of lesions in liver samples generated by the HIFU with varied acoustic pressures and with varied pulse lengths, respectively. Similar to the observations in the gel phantom, it is obvious that larger lesions could be generated in liver samples exposed to HIFU with larger acoustic pressure or longer pulse length.

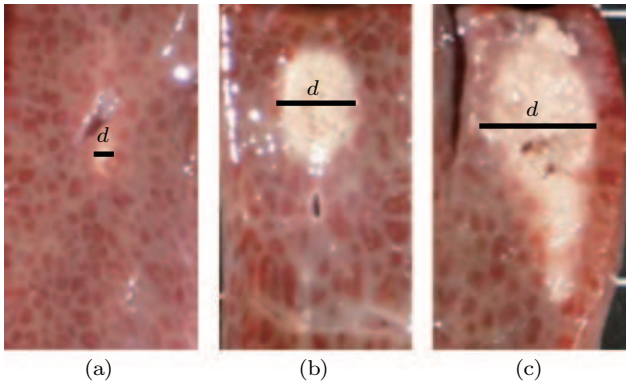


Fig. 6. (color online) Longitudinal cross-section images of the lesions in liver samples exposed to HIFU with the fixed pulse length 2000 cycles and varied acoustic pressures: (a) 7.5 MPa, (b) 8.75 MPa, and (c) 9.92 MPa.

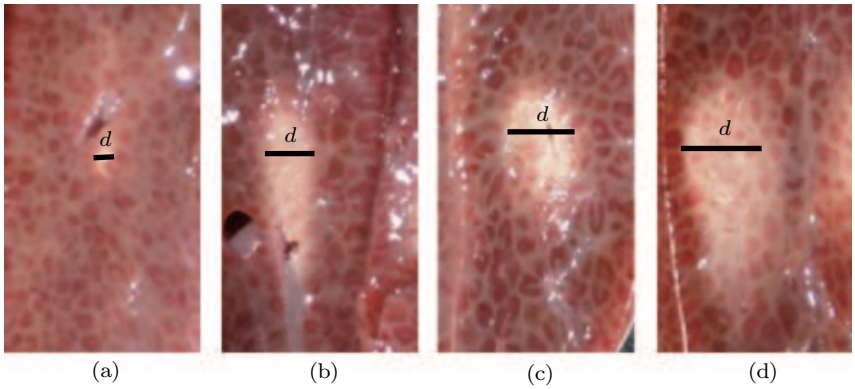


Fig. 7. (color online) Longitudinal cross-section images of the lesions in liver samples exposed to HIFU with the fixed acoustic pressure of 7.5 MPa and varied pulse lengths: (a) 2000 cycles, (b) 3000 cycles, (c) 4000 cycles, and (d) 6000 cycles.

To quantitatively investigate the change of lesion area with the ultrasonic exciting parameters, the lesion areas of the longitudinal and lateral cross-section generated by HIFU exposures are plotted in Fig. 8, as the functions of acoustic pressure and pulse length, respectively. It should be pointed out that the cross-section area in the longitudinal direction was quantified directly according to Figs. 6 and 7, while the lateral lesion area was deduced according to the estimated diameter d. In Fig. 8(a), both the calculated and measured lateral cross-section area of the lesion gradually rose with the increase of the acoustic pressure amplitude from 7.5 to 9.92 MPa, and the curves of lateral cross-section area versus acoustic pulse length exhibit the similar trend in Fig. 8(b). Moreover, compared with the lesions in gel (Fig. 5), it is found that larger lesions can be induced in a liver sample under the same acoustic exciting parameters, because liver tissue has higher acoustic speed and smaller specific heat. Furthermore, it is obvious that the longitudinal lesion shows more significant than the lateral lesion, which is similar to the results shown in Fig. 5.

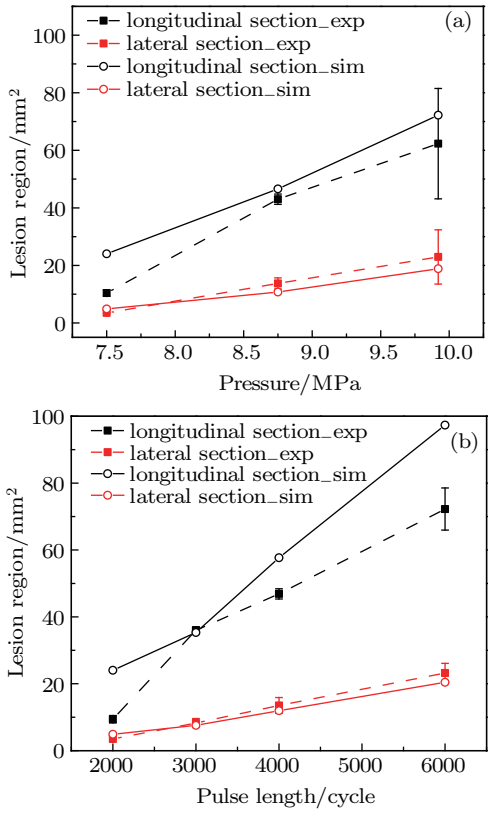


Fig. 8. (color online) Calculated and measured lesion area in liver samples. Lateral and longitudinal lesion area generated by HIFU (a) with varied acoustic pressure and the fixed pulse length of 2000 cycles, and (b) with varied pulse length and fixed acoustic pressure of 7.5 MPa.

3.3. Impact of cavitation on the lesion formation

Previous work has shown that the formation of HIFU-induced thermal lesion could be influenced by various factors. For instance, different shapes of lesion could be generated at varied acoustic pressures.[34] Here, by combining the observations in Figs. 3–8, one can conclude that a larger lesion could be formed both in the gel phantom and in *ex vivo* liver sample exposed to HIFU with larger pressure and longer pulse length, which is consistent with previous reports. However, it is interesting to notice that in Figs. 5 and 8 the measured areas of lesions in the lateral direction are generally comparable to the simulated data based on KZK and Pennes bioheat equations, while much larger discrepancy can be observed between the experimental and calculated results for the lesion areas in the longitudinal direction. Since it has been claimed in a previous study that cavitation may play an important role in lesion formation[5–9] although the cavitation-relative bio-effect is usually ignored in the theoretical modeling work, it is speculated that the discrepancy between the experimental and simulated results, especially in the evaluation of longitudinal lesion cross-section, could be ascribed to HIFU-induced cavitation activity. In order to verify this hypothesis, the temporal evaluation of the hyperechoic region in a B-mode image, which could be used as the indicator of the HIFU-induced cavitation bubble activity, was visualized in real-time by using a B-mode monitoring system.[35] As shown in Fig. 9, the maximum cavitation bubble areas generated in both gel and liver samples are quantified in terms of pixels and plotted as the functions of acoustic pressure and pulse length. It is obvious that the generation of cavitation bubbles is significantly enhanced by

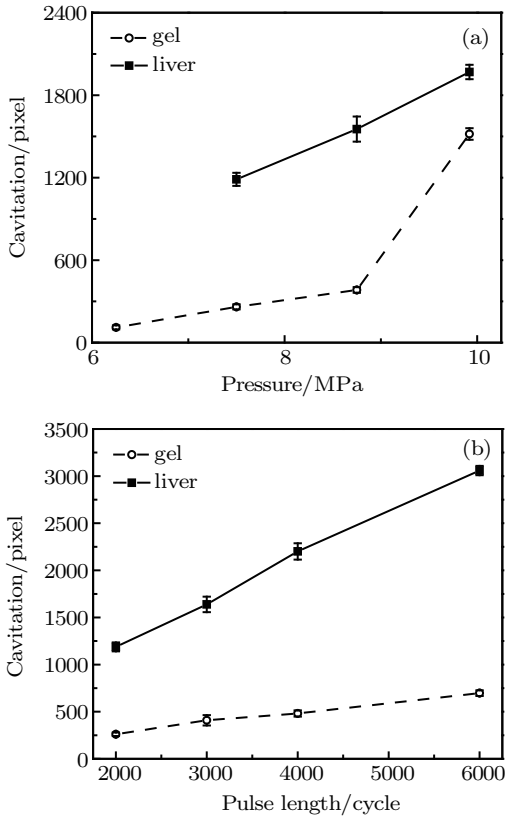


Fig. 9. The HIFU-induced cavitation activity in gel and liver samples. The maximum area of cavitation bubbles in terms of pixel (a) with varied acoustic pressure and the fixed pulse length of 2000 cycles, and (b) with varied pulse length and fixed acoustic pressure of 7.5 MPa.

increasing the acoustic pressure and pulse length due to the raised acoustic energy deposition, and much more intensified cavitation activity can be observed in liver samples than in gel phantom which might be attributed to the inhomogeneity of liver samples.

Furthermore, statistical analysis was performed for the pooled data to investigate the impact of HIFU-induced cavitation activity on the absolute discrepancy between simulated and measured lesion areas in both longitudinal and lateral directions. As shown in Fig. 10, the deviation of longitudinal lesion cross-section exhibits an approximately linear correlation with the enhanced cavitation activity with a Pearson coefficient of 0.79, while the lesion formation in the lateral direction is less correlated with HIFU-induced cavitation intensity.

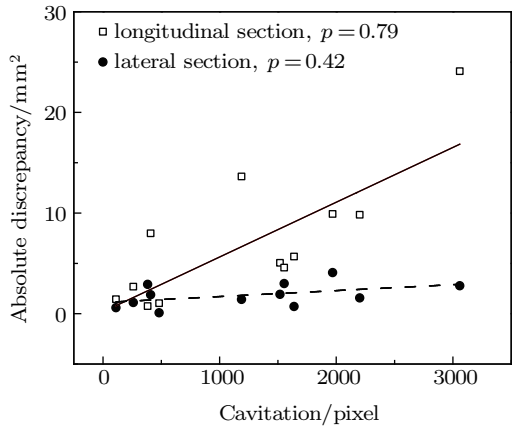


Fig. 10. The correlation between cavitation and the absolute discrepancy between the measured lesion area and the calculated one.

To get in-depth understanding of the influence of HIFU-induced cavitation on the lesion formation, the temperature elevation in gel at the HIFU focus was also investigated both experimentally and numerically. Figure 11 shows the calculated and measured temperature values at HIFU focus in gel with varied acoustic pressure amplitude and with varied pulse length, respectively. It is noticed that the results of HIFU-induced temperature elevation exhibit a similar trend as those demonstrated for the longitudinal lesion formation at various acoustic parameters (Fig. 5), which agrees with previous reports that the lesion formation should be highly dependent on HIFU-induced heat deposition.[5–9] As shown in Figs. 5 and 11, the measured data are initially greater than the simulated ones when the acoustic pressure increases from 6.25 to 8.75 MPa or the acoustic pulse length increases from 2000 to 4000 cycles, then turn over to be lower than the simulated values as the acoustic pressure keeps increasing to 9.92 MPa or the acoustic pulse length is further raised to 6000 cycles. Considering HIFU-induced cavitation activity can be intensified by the increasing acoustic driving parameters (Fig. 9), the initial superior trend demonstrated by the measured data could be explained by previous investigations that the presence of acoustic cavitation at the ultrasound focal region can lead to a substantially higher tissue heating rate.[6,8] In addition, one important observation which should be emphasized here is that, as the acoustic driving parameters exceed a certain level, HIFU-induced temperature elevation and lesion formation could be impaired by the enhanced cavitation bubble activity that might block the acoustic wave propagation and attenuate the delivery of acoustic energy to a targeted region.

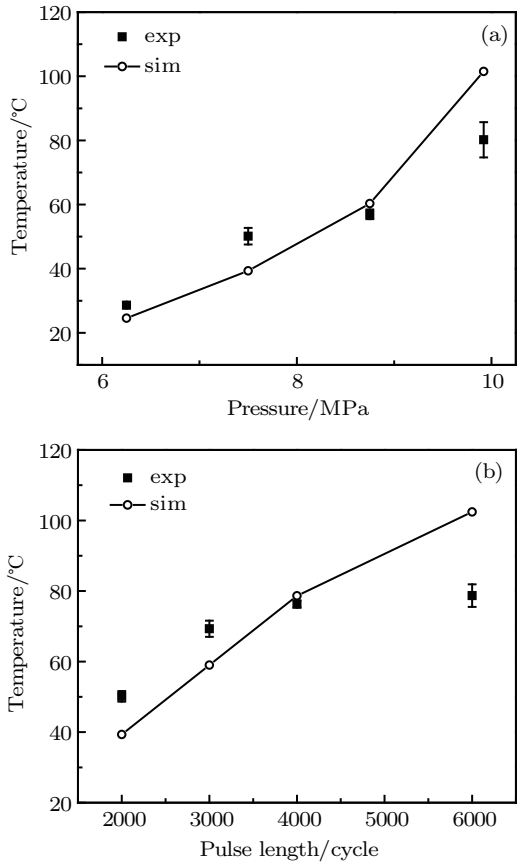


Fig. 11. Measured and calculated temperature values at the focus in gel (a) as a function of the acoustic pressure amplitude with a fixed pulse length of 2000 cycles, and (b) as a function of the pulse length with a fixed acoustic pressure of 7.5 MPa.

The *ex vivo* temperature study was not performed because it was too difficult to locate the thermal couple right at the HIFU focus in an opaque liver sample and make accurate measurement for HIFU-induced temperature changes. Nevertheless, the *ex vivo* studies on the longitudinal lesion area and cavitation bubble activity (Figs. 8 and 9) also can provide proofs for the hypothesis that excessive cavitation might be harmful to HIFU-induced tissue heating and lesion formation. One can notice that in Fig. 8 the measured longitudinal lesion areas are always less than the simulated results, since the cavitation activity generated in liver samples are much stronger than that in gel phantoms as shown in Fig. 9.

4. Conclusion

The effect of the cavitation on the lesion formation in gel and *ex vivo* liver tissue samples was investigated both theoretically and experimentally with respect to varied acoustic exciting parameters, such as the acoustic pressure amplitude and the pulse length. The thermal-induced lesion was modeled by the combination of the KZK equation and bio-heat equation, while the cavitation was quantitatively measured by use of the B-mode imaging. The results demonstrated that (i) larger acoustic pressure or longer pulse length could generate higher temperature at focus, which tends to create a larger lesion; (ii) the longitudinal lesion formation could be significantly affected by HIFU-induced cavitation bubbles, while the lateral lesion formation should be less dependent on cavitation activity, so that it is easier to be simulated using a theoretical model; (iii) excessive cavitation activity might be harmful to HIFU-induced tissue heating and lesion formation, which might induce uncontrollable bioeffects in HIFU treatment. The results obtained in the present work might provide better understanding of the impact of cavitation activity on HIFU-induced lesion formation, which should be important for achieving safer and more effective HIFU treatment.

References

[1] Chen T, Qiu Y Y, Fan T B and Zhang D 2013 *Chin. Phys. Lett.* **30** 074302
[2] Miller M W, Everbach E C, Miller W M and Battaglia L F 2003 *Ultrasound Med. Biol.* **29** 93
[3] Zhang L, Wang X D, Liu X Z and Gong X F 2015 *Chin. Phys. B* **24** 014301
[4] Holland C K and Apfel R E 1990 *J. Acoust. Soc. Am.* **88** 2059
[5] Hynynen K 1991 *Ultrasound Med. Biol.* **17** 157
[6] Holt R G and Roy R A 2001 *Ultrasound Med. Biol.* **27** 1399
[7] Miller D L and Gies R A 1998 *Ultrasound Med. Biol.* **24** 123
[8] Chen W S, Lafon C, Matula T J, Vaezy S and Crum L A 2003 *Acoust. Res. Lett. Onl.* **4** 41
[9] Farny C H 2007 *Diss. Abstr. Int.* **67** 7122
[10] Khokhlova V A 2006 *J. Acoust. Soc. Am.* **119** 1834
[11] Thomas H, Everett I V, Lee K W, Wilson E W, Guerra J M, Varosy P D and Olgin J E 2009 *J. Cardiovasc. Electrophysiol.* **20** 325
[12] Yu J, Chen C Y, Chen G, Guo X S, Ma Y, Tu J and Zhang D 2014 *Chin. Phys. Lett.* **31** 034302
[13] Fan T B, Liu Z B, Zhang D and Tang M X 2013 *IEEE T. Biomed. Eng.* **60** 763
[14] Zhang Z, Chen T and Zhang D 2013 *Chin. Phys. Lett.* **30** 024302
[15] Zhang C B, Liu Z, Guo X S and Zhang D 2011 *Chin. Phys. B* **20** 024301
[16] Qiu Y, Luo Y, Zhang Y, Cui W C, Zhang D, Wu J R, Zhang J F and Tu J 2010 *J. Control. Release* **145** 40
[17] N'Djin W A, Chapelon J Y and Melodelima D 2015 *PLoS One* **10** 0137317
[18] Kovatcheva R D, Vlahov J D, Stoinov J I and Zaletel K 2015 *Radiology* **276** 597
[19] Phukpattaranont P and Ebbini E S 2003 *IEEE Trans. Ultrason. Ferroelectr. Freq. Control* **50** 987
[20] Anand A and Kaczkowski P J 2004 *Arlo* **5** 88
[21] Souchon R, Soualmi L, Bertrand M, Chapelon J Y, Kallel F and Ophir J 2002 *Ultrasonics* **40** 867
[22] Kim H R, Dong G Y, Park S J, Choi K S, Um W, Kim J H, Park J H and Kim Y S 2016 *Mol. Pharm.* **13** 1528
[23] Kim Y S, Lim H K and Rhim H 2016 *PLoS One* **11** 0155670
[24] Mohsen H and Mehran J 2009 *International Conference on Information Technology: New Generation* p. 1468
[25] Filonenko E A and Khohlova V A 2001 *Acoust. Phys.* **47** 541
[26] Zhao X and Mcgough R J 2014 *IEEE International Ultrasonics Symposium* **3** 2225
[27] Canney M S, Bailey M R, Crum L A, Khokhlova V A and Sapozhnikov O A 2008 *J. Acoust. Soc. Am.* **124** 2406
[28] Khokhlova T D, Canney M S, Lee D, Marro K I, Crum L A, Khokhlova V A and Bailey M R 2009 *J. Acoust. Soc. Am.* **125** 2420
[29] Pennes H H 1948 *J. Appl. Phys.* **1** 93
[30] Sapareto S A and Dewey W C 1984 *Int. J. Radiat. Oncol.* **10** 787
[31] He B 1999 *IEEE Trans. Ultrason. Ferroelectr. Freq. Control* **46** 706
[32] Lafon C, Zderic V, Noble M L, Yuen J C, Kaczkowski P J, Sapozhnikov O A, Chavrier F, Crum L A and Vaezy S 2005 *Ultrasound Med. Biol.* **31** 1383
[33] Takegami K, Kaneko Y, Watanabe T, Maruyama T, Matsumoto Y and Nagawa H 2004 *Ultrasound Med. Biol.* **30** 1419
[34] Jensen C R, Ritchie R W, Gyöngy M, Collin J R T, Leslie T and Coussios C C 2012 *Radiology* **262** 252
[35] Rabkin B, Zderic V and Vaezy S 2005 *Ultrasound Med. Biol.* **31** 947